

Hydrodynamics of compressible superfluids in confined geometries

Abdul N Malmi-Kakkada¹, Oriol T Valls¹, Chandan Dasgupta²

¹School of Physics and Astronomy, University of Minnesota, Minneapolis, Minnesota 55455

²Centre for Condensed Matter Theory, Department of Physics, Indian Institute of Science, Bangalore 560012, India

Abstract. We present a study of the hydrodynamics of compressible superfluids in confined geometries. We use a perturbative procedure in terms of the dimensionless expansion parameter $(v/v_s)^2$ where v is the typical speed of the flow and v_s the speed of sound. A zero value of this parameter corresponds to the incompressible limit. We apply the procedure to two specific problems: the case of a trapped superfluid with a gaussian profile of the local density, and that of a superfluid confined in a rotating obstructed cylinder. We find that the corrections due to finite compressibility which are, as expected, negligible for liquid He, are important but amenable to the perturbative treatment for typical ultracold atomic systems.

PACS numbers: 47.37.+q, 67.25.bf, 67.85.De, 47.27.nd

1. Introduction

The hydrodynamics of superfluids confined in containers or channels of complex geometry is relevant to a variety of experimentally studied systems. The absence of friction in a superfluid and the irrotational nature of superfluid flow (in the absence of vortices) lead to a variety of unusual hydrodynamic effects that depend crucially on the confining geometry.

A large number of experimental investigations into superfluidity in trapped, ultracold atomic systems [1, 2, 3] have been carried out in recent years. Various signatures of superfluidity, such as persistent flow, reduction in the moment of inertia due to the frictionless nature of the superfluid (the so-called non-classical rotational inertia (NCRI)) and formation of quantized vortices have been observed in both bosonic [4, 5, 6, 7] and fermionic [8] systems. In all these experiments, the superfluid is confined in a small region by an external trapping potential. While the early experiments on such systems were carried out for traps with simple geometry, more recent ones have begun to explore the properties of superfluid condensates in traps with a more complex structure. Superfluid flow in a toroidal trap has been observed [6], and the effects of a repulsive optical barrier that tends to block the superflow have been investigated in recent experiments [9, 10]. Studies of superfluid hydrodynamics in containers with complex geometry are obviously relevant for understanding the results of experiments on superfluidity in atomic systems confined in such traps.

Motivation for studies of superfluid hydrodynamics in confined geometries is also provided by reports [11, 12] of an abrupt change in the resonant period of a torsional oscillator filled with solid ^4He , initially interpreted as NCRI in solid ^4He , at sufficiently low temperatures. While the interpretation is controversial [13], a possible explanation [14, 15, 16, 17] is that superfluidity occurs in solid ^4He along extended crystal defects such as dislocation lines and grain boundaries which form complex disordered structures. Studies of the flow properties of a superfluid confined in channels and networks of irregular geometry are obviously useful for assessing the validity of such theories.

The hydrodynamics of superfluids confined in containers of simple geometries, such as spherical, cylindrical or rectangular, has been studied extensively [18, 19] in the past. These studies, all in the incompressible limit, were recently extended [20] by two of us to more complex geometries, such as wedges and blocked rings, both in the case where there are no vortices (so that the superfluid flow is irrotational) and the case where a single vortex was present. The same authors carried out a study [17] on the effects of superfluidity along grain boundaries in a two-dimensional bosonic system. While the results of these studies could be applied to experiments involving superfluid ^4He , they were not directly applicable to cold atomic systems because of the incompressibility assumption. This assumption constrains the local density in equilibrium to be uniform throughout the system. While this is an extremely good approximation for superfluid ^4He , it is not a good one for cold atomic systems in which the presence of a confining potential causes the equilibrium density to be substantially inhomogeneous. This inhomogeneity has significant effects on the superfluid properties of the confined atomic system, as found in both experimental [1] and theoretical [21, 22] investigations. Therefore, it was doubtful if the results of these earlier studies [17, 20] would be valid for cold atomic systems. For example, calculations in Ref. [20] showed that the velocity field for a superfluid confined in a two-dimensional wedge with opening angle $\beta > \pi$ diverges at the tip of the wedge for *any* nonzero value of the angular velocity Ω of the wedge about an axis perpendicular to it and passing through its tip. This divergence could be removed by the nucleation of a single vortex. This implies that either a normal region near the tip of the wedge or a vortex must be present for any nonzero value of Ω . The size of the region near the tip where the velocity exceeds the critical velocity was estimated to be too small to be experimentally observable for liquid ^4He , but it was found that it may be observable in cold atomic systems. However, the validity of the results for cold atomic systems could not be established because the calculation was carried out for an incompressible superfluid. In general, firm conclusions for cold atomic systems cannot be drawn from hydrodynamic calculations performed under the assumption of incompressibility and uniform equilibrium density. Clearly, a method in which this assumption is removed is needed for studies of the hydrodynamics of these systems.

To accomplish this purpose, we start, in this paper, with the hydrodynamic equations for a compressible superfluid. Although the effect of compressibility in cold atomic systems has been studied via the Gross-Pitaevskii (GP) equation [22, 23], it is simpler for our purpose of perturbatively studying the compressibility corrections, to start directly with the hydrodynamic limit and the associated coarse grained equations based on conservation of mass and momentum. The hydrodynamic equations we consider can be obtained [22, 23] from the GP equation if a quantum stress term, known [24] to be unimportant in the hydrodynamic regime, is neglected. The procedure we use to solve the hydrodynamic equations is based on an expansion in

parameter $(v/v_s)^2$, the square of the Mach number, where v is some characteristic speed of the problem and v_s is the speed of sound. Such expansions have been previously used [25, 26] in other quantum fluids problems. Our expansion procedure leads to linear differential equations, which makes it much easier to find analytic solutions: this is a considerable advantage of our method. At zeroth order in this small parameter one recovers the incompressible results, since v_s is then formally infinite. Our expansion, as it will be seen, is particularly convenient to the study of situations where a flow is imposed on the system by external means. We then proceed to apply this procedure to two specific situations in this category. Although these have been chosen largely because analytic solutions in the incompressible limit can either be easily obtained or already exist, both of these situations have been realized in experiments on cold atomic systems. In the first case, we assume that external constraints confine the superfluid in such a way as to produce a gaussian profile for the local density of the stationary superfluid, a situation similar to that considered experimentally in Ref. [27] and theoretically in Refs. [21, 28]. The specific force fields required to establish this distribution drop out of the equations: only the resulting density distribution matters. We then, for this example, assume that a flow corresponding to one quantum of axial circulation (i.e. a single vortex) is established in such a way that it is a solution of the zeroth order hydrodynamic equations, and evaluate the first order corrections to the velocity field and to the density due to finite compressibility. In the second problem we consider afresh the obstructed cylinder situation previously studied [20] in the incompressible limit and again evaluate the first order corrections to both components of the velocity field, and to the density, due to the finite compressibility. The geometry considered here is similar to that of recent experiments [9, 10] on Bose-Einstein condensates in a toroidal trap with a repulsive barrier. In both cases we find, as expected, that the corrections are vanishingly small for liquid He. On the other hand, we find that for typical cold atomic systems the corrections due to finite compressibility are often not negligible but that they are sufficiently small to be amenable to our perturbative solution. The observation that corrections due to finite compressibility in cold atomic systems in the hydrodynamic regime are amenable to perturbative solution for the two widely different problems considered here is interesting because it suggests that similar perturbative treatments would be possible for other problems of interest in studies of superfluidity in cold atomic systems.

The rest of this paper is organized as follows. In section 2, we present the details of the perturbative method of calculation used here. The results obtained from application of this method to the problems mentioned above are described in detail in section 3. Section 4 contains a summary of the main results and concluding remarks.

2. Methods

As explained above, our objective is to study the effect of compressibility on superfluid hydrodynamics in confined geometries, starting with the results for incompressible fluids. The behavior of compressible normal liquids has been studied as early as 1883 [29]. Starting with the general equations governing inviscid fluid flow - the continuity and Euler equations - we use a perturbative method to study the effect of finite compressibility in the limit where the perturbation parameter, while low, is nonzero. We will see that this is a realistic limit for cold atomic systems of

experimental interest. Our perturbative method has similarities to that used in Ref. [30]. That study focuses on the propagation of sound waves, a limit where the perturbation parameter cannot be assumed to be much smaller than unity. The small dimensionless parameter associated with the perturbative expansion is the Mach number, the ratio of the characteristic fluid velocity to the sound speed. For quantum systems, such expansions have been used earlier in Ref. [25, 26] which address a very different problem of the critical speed for the nucleation of vortices in superfluid flow around a disk as compared to our present work on flow patterns for superfluids in confined geometries. The procedure will be illustrated by calculating, for two examples of confined superfluids, the corrections to the velocity field and the density distribution in the low temperature limit where viscosity effects can be neglected.

2.1. General

As a simpler alternative to deriving the equations of compressible superfluid hydrodynamics via the GP equation, we start with the fundamental hydrodynamic equations governing fluid flow in the steady state i.e. mass conservation as given by the continuity equation:

$$\nabla \cdot (\rho \vec{v}) = (\nabla \rho) \cdot \vec{v} + \rho(\nabla \cdot \vec{v}) = 0 \quad (1)$$

and momentum conservation as given by the Euler equation:

$$(\vec{v} \cdot \nabla) \vec{v} = -\frac{\nabla p}{\rho} + \frac{\vec{f}}{\rho} \quad (2)$$

where ρ is the mass density, \vec{v} represents the velocity field, p the pressure, and \vec{f} is the external force per unit volume. The steady state assumption means, as usual, that we are averaging over microscopic scale time fluctuations. Hydrodynamics can also be derived by starting from microscopic or quasi microscopic equations of motion and then coarse graining. When one does that from the GP equations [22, 23, 25, 26] one obtains in the Euler equation an additional quantum stress term. This term need not be included here for two reasons: first, as explained on page 170 of Ref. [23] (see also Ref. [24]) the order of magnitude of this term (which involves third derivatives of the density) is down by a factor of $(\ell/L)^2$ where ℓ is a microscopic quantum length and L the characteristic length associated with macroscopic pressure variations: it is hence negligible for the hydrodynamic problems considered here. Secondly, this term (involving as it does density derivatives) vanishes at $\kappa = 0$ and, since it appears in the same way as the term \vec{f} , it would similarly acquire an explicit factor of κ in Eq. (3) below. It is therefore a second or higher order correction in our small parameter. Short range fluctuations may exist, just as they do in classical fluids, but they are averaged over the macroscopic distance L in the hydrodynamic limit. Such a scale clearly exists in experimental Bose systems: the Thomas-Fermi radius of trapped Bose gases can be between two or three orders of magnitude larger than the microscopic coherence length. From experiments on superfluid flow in Bose systems [4, 31, 32] it can be seen that the characteristic Mach number squared, our dimensionless expansion parameter $(v/v_s)^2$, is of order $10^{-2} - 10^{-4}$ and hence small in these systems. The Thomas-Fermi approximation predicts an abrupt drop to zero in the density of the condensate beyond the Thomas-Fermi radius, but this is an artifact of the Thomas-Fermi method: the actual variation in density is smoother. This does not affect the validity of our approach just as the abrupt density drop near a wall does not invalidate

classical hydrodynamics given that a large region over which the parameter $(v/v_s)^2$ is small exists.

We consider ρ to be a function of p only (barotropic limit). This limit applies[33] in the very low temperature case that we study: at zero temperature p can only be a function of ρ . Using the definition of compressibility ($\kappa = \frac{1}{\rho} \frac{\partial \rho}{\partial p}$), Eq.(2) becomes:

$$\rho^2 \kappa (\vec{v} \cdot \nabla) \vec{v} = -\nabla \rho + \rho \kappa \vec{f}. \quad (3)$$

We now start the perturbative calculation by writing:

$$\rho = \rho_0 + \rho_1 \quad (4)$$

$$\vec{v} = \vec{v}_0 + \vec{v}_1 \quad (5)$$

where the zero index denotes quantities in the incompressible ($\kappa = 0$) limit and the index one in v_1, ρ_1 denotes the changes in velocity field and density distribution due to the finite compressibility. Substituting Eqs. (4) and (5) into Eqs (1) and (2), the Euler equation at zeroth order takes the form:

$$\nabla \rho_0 = \rho_0 \kappa \vec{f} \quad (6)$$

which reflects the fact that at $\kappa = 0$ it would take an infinite force to induce a density gradient (here and below, we consider the product κf to be finite, of order unity). For future convenience, let us assume that such a density gradient has somehow been induced by external means. In that case the zero order continuity equation would take the form:

$$(\nabla \rho_0) \cdot \vec{v}_0 + \rho_0 (\nabla \cdot \vec{v}_0) \equiv \mathcal{D}^0 \vec{v}_0 = 0, \quad (7)$$

which reduces to the usual form $\nabla \cdot \vec{v}_0 = 0$ in the absence of external forces. Here we have introduced the operator:

$$\mathcal{D}^0 \equiv \rho_0 (\nabla) \cdot + (\nabla \rho_0) \cdot. \quad (8)$$

Proceeding now to first order, the corresponding terms in the continuity equation yield:

$$-(\nabla \rho_1) \cdot \vec{v}_0 = \mathcal{D}^0 \vec{v}_1 + \rho_1 (\nabla \cdot \vec{v}_0) \quad (9)$$

while from those in the Euler equation we have:

$$\rho_0^2 \kappa (\vec{v}_0 \cdot \nabla) \vec{v}_0 = -\nabla \rho_1 + \rho_1 \kappa \vec{f}. \quad (10)$$

Taking the scalar product of Eq. (10) with \vec{v}_0 and making use of Eqs. (9) and (7) one obtains:

$$\mathcal{D}^0 \vec{v}_1 = \rho_0^2 \kappa \vec{v}_0 \cdot (\vec{v}_0 \cdot \nabla) \vec{v}_0. \quad (11)$$

By this procedure the external force has been eliminated from the equations. The reason this is possible is that the only role of the force is to impose the zeroth order density profile, ρ_0 , which alone has physical meaning. Eqns. (7), (9) and (11) are the basic set of equations needed. In general, the best course to obtain the first order results, after getting the zeroth order solution, is to solve first Eq. (11) and then obtain the first order density profile from Eq. (9).

We now verify the physical meaning of the dimensionless perturbation parameter associated with the low compressibility limit, as discussed above. Dividing through Eq. (10) by ρ_0 , introducing the average speed of sound v_s via $\rho_0 \kappa = v_s^{-2}$ and

introducing the dimensionless variable $\tilde{\rho} \equiv \rho_1/\rho_0$ (i.e. the dimensionless density correction) we have:

$$-\nabla\tilde{\rho}_1 + \tilde{\rho}_1\kappa\vec{f} = \left(\frac{\vec{v}_0}{v_s} \cdot \nabla\right)\frac{\vec{v}_0}{v_s}, \quad (12)$$

where we recall that the product κf must be viewed as finite. We see from this result that the dimensionless perturbation parameter associated with the correction to the density due to compressibility is indeed of order $(v_0/v_s)^2$. Proceeding in a similar way to evaluate the order of magnitude of the correction to the velocity (\vec{v}_1) due to the finite compressibility, it can be seen that the dimensionless perturbation parameter associated with the correction to velocity field (\vec{v}_1) is $\lambda \equiv (v_0/v_s)^2$.

2.2. Zero applied force

As explained above, the equations obtained from the perturbative analysis are quite general and can be used when $\rho_0(r)$ is uniform, as well as when it takes on a specific inhomogeneous form due to the application of some external force \vec{f} which need not be specified. In the case where no external force is imposed on the fluid, the zeroth order density distribution is of course a constant. This applies to the calculations performed in Ref. [20], for an obstructed annular cylinder as explained in the Introduction. In this case it is more convenient to start by simplifying the basic equations from the beginning. Since $\nabla\rho_0 = 0$ and $\nabla \cdot \vec{v}_0 = 0$, one has for the continuity equation at first order:

$$(\nabla\rho_1) \cdot \vec{v}_0 + \rho_0(\nabla \cdot \vec{v}_1) = 0. \quad (13)$$

In this limit the first order Euler equation Eq. (10) is:

$$-\nabla\rho_1 = \rho_0^2\kappa(\vec{v}_0 \cdot \nabla)\vec{v}_0 \quad (14)$$

Combining the two equations above, we obtain the following equation for \vec{v}_1 :

$$\nabla \cdot \vec{v}_1 = \rho_0\kappa\vec{v}_0 \cdot (\vec{v}_0 \cdot \nabla)\vec{v}_0 \quad (15)$$

with the right side known from the solution of the zeroth order equations. Since one of these equations is $\nabla \cdot \vec{v}_0 = 0$, similar Green function methods lead to solutions for both \vec{v}_0 and \vec{v}_1 . Specializing to the curl free case (absence of vortices) we introduce a scalar potential, $V(\vec{r})$, such that $\vec{v}_1(\vec{r}) = \nabla V(\vec{r})$. Eq. (15) then becomes:

$$\nabla^2 V = \rho_0\kappa\vec{v}_0 \cdot (\vec{v}_0 \cdot \nabla)\vec{v}_0, \quad (16)$$

which we solve by finding the appropriate Green function with specified boundary conditions. Once this is done we solve for \vec{v}_1 from:

$$V(\vec{r}) = \int d\vec{r}' G(\vec{r}', \vec{r}) \rho_0\kappa\vec{v}_0 \cdot (\vec{v}_0 \cdot \nabla)\vec{v}_0 \quad (17)$$

recalling that $\vec{v}_1 = \nabla V(\vec{r})$. The correction to the density profile due to nonzero compressibility - ρ_1 - is calculated from Eq. (14) using the result for \vec{v}_0 obtained from solving the equation $\nabla \cdot \vec{v}_0 = 0$.

We conclude this general discussion with a brief discussion of the relation of our method to the Thomas-Fermi approximation. Eqn. (6) is an equilibrium relation ($v = 0$) and in that respect it is analogous to neglecting the kinetic terms in the GP equation: in this sense it resembles the Thomas-Fermi approximation in equilibrium. Corrections to the equilibrium Thomas-Fermi approximation have been studied previously. For example, Ref. [34] keeps terms linear in the velocity in the context of studying collective modes. This is different from our current study where, as explained in the Introduction, we consider induced flows.

3. Results

In this section we present the results of calculations of the corrections to the velocity field (\vec{v}_1) and density (ρ_1) due to finite compressibility using the perturbative method described in the section above. We study the effect of nonzero compressibility on the velocity field and density distribution of confined superfluids in two different situations. In the first case, an external force imposed on the fluid leads to an equilibrium gaussian density profile. The other case, in the $f = 0$ limit, deals with the compressibility corrections for superfluid flow in an obstructed cylinder, as discussed in Ref. [20]. In the case of an obstructed cylinder, the fluid is driven by an obstruction and therefore the Thomas-Fermi approximation is not valid as the kinetic energy term cannot be neglected.

3.1. Gaussian density profile

We consider first the case of a cylindrical sample where an external force imposed on the fluid in equilibrium results in a gaussian density profile i.e.

$$\rho_0(r) = \rho_a e^{-(\frac{r}{\sigma})^2} \quad (18)$$

where σ is the characteristic length scale associated with the density profile and r the cylindrical radial coordinate. We assume the cylinder is long enough so that we can neglect edge effects and solve the problem as a quasi two-dimensional one. Density profiles other than a gaussian can also be considered by the same method: here we focus on this case as an example. In order to calculate ρ_1 and \vec{v}_1 we use equations (9) and (11) respectively, which requires us to calculate first an appropriate zeroth order velocity field \vec{v}_0 corresponding to the incompressible limit.

To calculate \vec{v}_0 , we use the zeroth order continuity equation (Eq. (7)) with the gaussian density profile, ρ_0 , specified above. Calculating $\nabla \rho_0$ and defining a velocity potential such that $\vec{v}_0 = \nabla V_0(r)$, Eq. (7) takes the form:

$$\nabla^2 V_0 = \frac{2r}{\sigma^2} \frac{\partial V_0}{\partial r}. \quad (19)$$

This equation has a variety of solutions reflecting the many possibilities for the velocity field. For our example, we restrict ourselves to begin with to the case where \vec{v}_0 has no azimuthal dependence. Assuming then a purely radial solution i.e. $V_0(r, \phi) = F(r)$ we obtain $\mathcal{D}_r^0 F(r) = 0$ where

$$\mathcal{D}_r^0 \equiv r \frac{\partial}{\partial r} + r^2 \frac{\partial^2}{\partial r^2} - \frac{r^3}{\sigma^2} \frac{\partial}{\partial r}. \quad (20)$$

The solution is:

$$F(r) = C_1 Ei((r/\sigma)^2) \quad (21)$$

where Ei is the usual exponential integral function. We obtain from this a purely radial part of v_0 namely:

$$\vec{v}_{0r} = \frac{C_1}{r} e^{(\frac{r}{\sigma})^2} \hat{r} \quad (22)$$

where the integration constant C_1 is a quantity with units of circulation. The increase in the velocity with r appears strange until one recalls that the density decreases (see Eq.(18)) exponentially so that the current decreases with r . To this particular solution we add an azimuthal component corresponding to a vortex centered at the origin. This

amounts to adding to the velocity potential a term proportional to ϕ , which of course also satisfies the linear Eq. (19). This leads to an azimuthal component:

$$\vec{v}_{0\phi} = \frac{C_2}{r} \hat{\phi} \quad (23)$$

Introducing this vortex in the fluid implies that the curl of the zeroth order velocity field, $\nabla \times \vec{v}_0 = 2\pi\delta(\vec{r})\hat{z}$ is non-zero. This does not contradict the definition of \vec{v}_0 as a gradient of a velocity potential since one is dealing with a singular field. The singularity at the origin requires the imposition of a small r cutoff. At the vortex core radius in a Bose fluid, the characteristic velocity of fluid flow is of the same order of magnitude as the sound velocity [22]. The region near the vortex core is also characterized by faster density variations, making the quantum pressure term important. Therefore, we introduce a short distance cutoff near the vortex of order few times the vortex core radius. Outside this region our assumptions of small Mach number squared and negligible quantum pressure term hold true. The circulation around the origin due to the azimuthal component of the velocity is $2\pi C_2$. Physically, we know that the circulation must be quantized. It follows that, as opposed to C_1 , C_2 is not a completely arbitrary constant, but must be an integer number of circulation quanta h/m . To make an estimate of the order of magnitude of the effect of nonzero compressibility, we assume in our numerical work that there is one quantum of circulation.

We now proceed to the first order calculation taking as our zeroth order results the density distribution Eq. (18) and the velocity field given by the sum of Eqs. (22) and (23). In the results presented in this subsection, we measure lengths in units of σ , and choose for our illustrative example $C_1 = C_2$. This choice of C_2 leads to some formal simplifications.

To evaluate the first order corrections, we now turn to Eq. (11) in order to solve for the correction to the velocity field (\vec{v}_1). We use the Green function method for this purpose. It is not hard to see that the azimuthal part of \vec{v}_0 does not contribute to the right side of Eq. (11). Hence it is sufficient to find the Green function corresponding to the operator \mathcal{D}_r^0 introduced in Eq. (20):

$$\mathcal{D}_r^0 G(r, r') = \frac{1}{r} \delta(r - r') \quad (24)$$

Solving the second order differential Eq. (24), we find this Green function to be:

$$G(r, r') = \frac{Ei(\frac{r_{>}^2}{\sigma^2})}{2} \quad (25)$$

where $r_{>}$ is the larger one of the two radial coordinates r, r' . Introducing then a velocity potential V_1 such that $\vec{v}_1 = \nabla V_1(r)$, Eq. (11) leads us to V_1 :

$$V_1 = \int r' dr' G(r, r') [\rho_0^2 \kappa \vec{v}_0 \cdot (\vec{v}_0 \cdot \nabla) \vec{v}_0] \quad (26)$$

Evaluating the expression on the right side of Eq.(26) with the Green function given above and the zeroth order velocity fields, we obtain analytically the potential associated with the correction to the velocity field (\vec{v}_1) due to nonzero compressibility. The quantity \vec{v}_1 itself can then be evaluated. As already anticipated in our zeroth order results, the divergence of the azimuthal field at $r = 0$ requires the introduction of a small r cutoff, which we denote as b . It is chosen as discussed above, which also ensures that v_0 does not exceed the critical velocity. The result for \vec{v}_1 is found to be:

$$\vec{v}_1 = \rho_a \kappa \frac{e^{s^2}}{r \sigma^2} \left[\frac{C_1^3}{2} (F_1(s^2, \delta^2)) - \frac{C_1 C_2^2}{2} (F_1(-s^2, -\delta^2) + 2(Ei(-\delta^2) - Ei(-s^2))) \right] \hat{r} \quad (27)$$

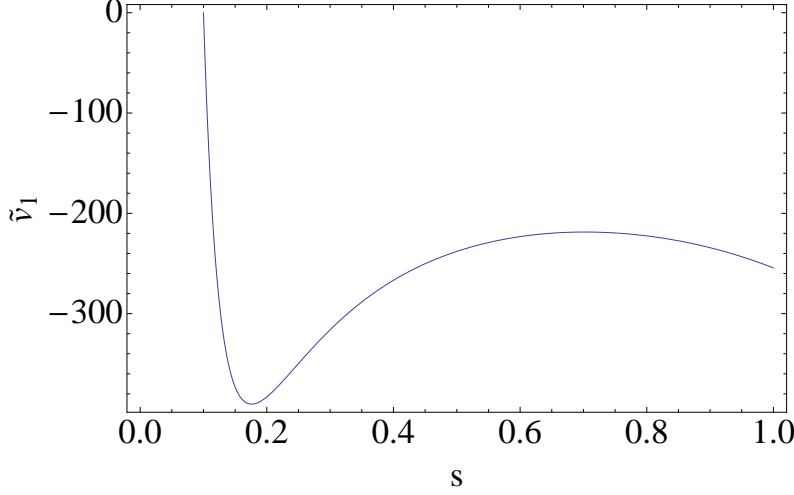


Figure 1. The dimensionless first order correction to the velocity field due to finite compressibility, plotted versus s . The quantity plotted, \tilde{v}_1 , is defined as $v_1/\lambda v$.

where we have introduced the dimensionless length $s \equiv r/\sigma$ and the dimensionless cutoff $\delta \equiv b/\sigma$. We have also introduced the auxiliary function F_1 as:

$$F_1(s^2, \delta^2) = -\frac{e^{\delta^2}}{\delta^2} + \frac{e^{s^2}}{s^2} - Ei(\delta^2) + Ei(s^2). \quad (28)$$

Although the zeroth order velocity has both radial and azimuthal components, the correction is purely radial. Nevertheless, the azimuthal component of \vec{v}_0 has a large effect on the result via the C_2^2 dependence of the second term in Eq. (27). When $C_1 = C_2$ it is possible to further simplify the result. Expressing in that case \vec{v}_1 in the natural dimensionless form, that is, in units of $C_1/\sigma \equiv v$ we have:

$$\frac{\vec{v}_1}{v} = \frac{1}{2} \left(\frac{v}{v_s} \right)^2 \frac{e^{s^2}}{s} (H(\delta) - H(s)) \hat{r}, \quad (29)$$

where $v_s^2 \equiv 1/\rho_a \kappa$ and the function $H(\xi)$ is defined as

$$H(\xi) = -\frac{e^{\xi^2}}{\xi^2} - \frac{e^{-\xi^2}}{\xi^2} - Ei(\xi^2) - Ei(-\xi^2). \quad (30)$$

In Eq. (29) the dimensionless perturbation parameter λ discussed above can be clearly identified as the prefactor appearing in the right side. Figure 1 shows the magnitude of the correction to the velocity, \tilde{v}_1 , in units of λv for the case where $C_1 = C_2$ as in Eq. (29). This quantity is plotted as a function of the dimensionless radial coordinate s . The value of the cutoff parameter has been set so that $\delta = 0.1$. The numbers in the vertical scale seem to be large. This can easily be seen (see Eq. (29)) to arise from the smallness of our choice for the cutoff parameter δ . We will see that in actual situations, the parameter λ is small enough so that the first order velocity correction is indeed much smaller than the zeroth order velocity scale. A similar remark applies to the density correction discussed below.

We can now study the correction to the density profile (ρ_1) and eventually to the physical current associated with fluid flow. Using Eq. (9) we find that a solution

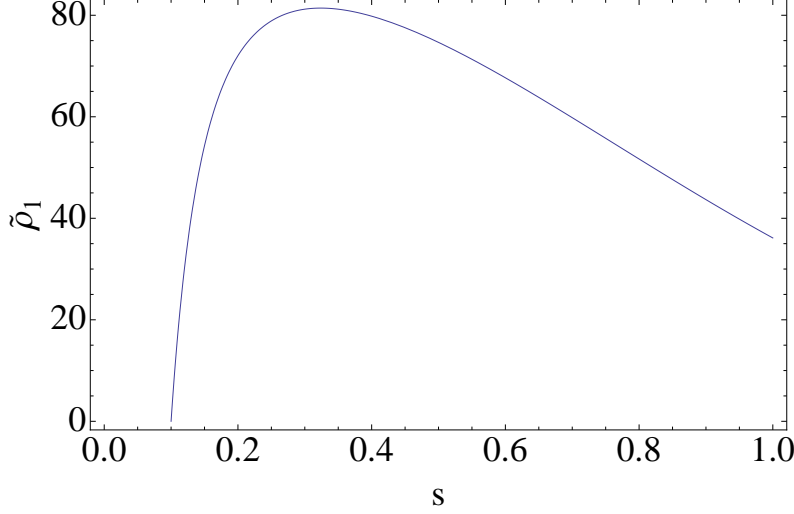


Figure 2. Plot of the dimensionless first order correction to the density due to finite compressibility versus s . The quantity plotted, $\widehat{\rho}_1$, is defined as $\rho_1/\lambda\rho_a$.

with azimuthal symmetry exists and satisfies the first order inhomogeneous differential equation:

$$-\frac{\partial\rho_1}{\partial r}(v_{0r}) = \rho_0\frac{\partial v_1}{\partial r} + \rho_1\left(\frac{\partial v_{0r}}{\partial r} + \frac{v_{0r}}{r}\right) + \frac{\partial\rho_0}{\partial r}v_{1r} \quad (31)$$

It is straightforward to solve this differential equation using the method of integrating factors, and we find the correction ρ_1 to the density to be:

$$\frac{\rho_1}{\lambda\rho_a} = \frac{e^{-s^2}}{2}(G_1(\delta) - G_1(s)) \quad (32)$$

where the function G_1 is defined as

$$G_1(\xi) = \frac{e^{-\xi^2}}{\xi^2} + \frac{e^{\xi^2}}{\xi^2} - 2\Gamma[0, -\xi^2] - 2\log(\xi^2) - Ei(\xi^2) + Ei(-\xi^2). \quad (33)$$

Here $\Gamma[a, z]$ represents the incomplete Gamma function. Figure 2 shows a plot of the first order correction to the density. The quantity plotted is the left side of Eq. (32) as a function of the dimensionless radial coordinate s for the same conditions as in Fig. 1.

We can now look at the corresponding current \vec{j} that is a characteristic physical property of the system. The total current is the sum of zeroth and first order terms: $\vec{j}_{total} = \vec{j}_0 + \vec{j}_1$, where $\vec{j}_0 = \rho_0\vec{v}_0$, and $\vec{j}_1 = \rho_0\vec{v}_1 + \rho_1\vec{v}_0$ is the first order correction. In Figure 3 we present a vector plot of \vec{j}_1 . The conditions, units and parameter values are as in Figs. 1 and 2. We see that the magnitude of the physical current arising from finite compressibility is more pronounced closer to the central region of the cylinder.

To check the validity of the perturbative treatment developed here, it is necessary to examine the order of magnitude of the perturbation parameter λ for typical cold atomic systems. We assume that C_2 corresponds to one quantum of circulation. Thus we take, as orders of magnitude, $\sigma \approx 10^{-5}m$ [27], $C_2 \approx 10^{-9}m^2/s$ and

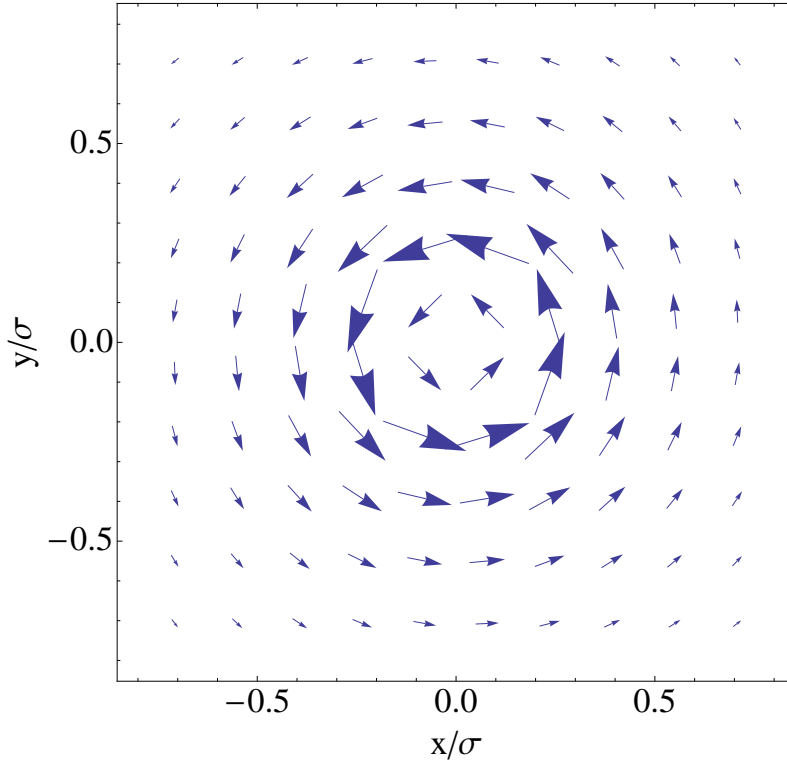


Figure 3. Vector plot of the first order correction to the current due to finite compressibility in the calculation described in subsection 3.1. Lengths are in units of σ and the parameters are as in Figs. 1 and 2.

[4, 31, 32, 35] $v_s \approx 10^{-2} m/s$. This leads to the estimate $\lambda \approx 10^{-4}$. Thus, for cold atomic systems, while λ may be quite small, the corrections are far from negligible since the quantities plotted in Figs. 1 and 2 can be as large as several hundreds. Thus, corrections up to the level of $\sim 10\%$ can easily arise. Hence, we conclude that compressibility effects in the hydrodynamics of cold atomic systems, as seen from the analytic perturbative method used here, cannot be neglected. For superfluid Helium, however, the circulation quantum is much larger (a factor of 20 compared to Rb), the speed of sound much larger [36] and system sizes also larger: thus a similar estimate yields $\lambda \approx 10^{-14}$ and the corrections are negligible, as expected.

3.2. Obstructed Cylinder

We now consider the second problem, which is perhaps of clearer physical relevance: we calculate the compressibility corrections for the obstructed rotating cylinder geometry studied in Ref. [20]. This geometry is that of a circular cylinder of radius a with a thin radial wall extending from the axis to the outer wall of the cylinder. We assume that the cylinder is long enough for end effects to be negligible. We define an angle ϕ from the line of obstruction so that $\phi = 0$ defines the location of the radial wall. In this case there is no applied force in equilibrium: thus when the cylinder does not rotate the density is uniform, at a value which we take as our unit of density. When the cylinder

rotates about its axis with angular speed Ω a velocity field is induced in it. In the zero compressibility limit, this velocity field is known[20]. We will calculate here the corrections to the velocity field and the density profile due to non-zero compressibility within the perturbative method described in Sec. 2. The field \vec{v}_0 for the geometry under consideration was obtained in Ref. [20] via both scalar and vector potential methods. It can be expressed in series form:

$$v_{0r}(r, \phi) = \Omega r \sin(2\phi) + \frac{16\Omega a}{\pi} \sum_{n \text{ odd}} \left(\frac{r}{a}\right)^{n/2-1} \frac{1}{n^2 - 16} \cos(n\phi/2) \quad (34)$$

$$v_{0\phi}(r, \phi) = \Omega r \cos(2\phi) - \frac{16\Omega a}{\pi} \sum_{n \text{ odd}} \left(\frac{r}{a}\right)^{n/2-1} \frac{1}{n^2 - 16} \sin(n\phi/2). \quad (35)$$

To obtain the correction to the zeroth order velocity field (\vec{v}_1) due to finite compressibility we solve Eq. (15) by the Green function method. We introduce a scalar velocity potential V_1 so that $\vec{v}_1(\mathbf{r}) = \nabla V_1(\mathbf{r})$, and calculate the Green function associated with the operator ∇^2 (see Eq. (16)) for appropriate boundary conditions. We recall[20] that the boundary condition on the total velocity field, $\mathbf{v}(\mathbf{r})_{\perp} = (\boldsymbol{\Omega} \times \mathbf{r})_{\perp}$, where \mathbf{r} is a vector from the center to a point on the boundary, and \perp denotes the component normal to the boundary, is already satisfied by the zeroth order velocity in Eq. (34). Hence, $V_1(\mathbf{r})$ satisfies zero Neumann boundary conditions at the cylinder surface. The Green function in this case is then found by standard procedures[37] with the result:

$$G(r, \phi; r', \phi') = -\frac{1}{\pi} \sum_{n=2}^{\infty} \frac{1}{n} r_{<}^{n/2} \left(\frac{1}{r_{>}^{n/2}} + \frac{r_{>}^{n/2}}{a^n} \right) \cos(n\phi/2) \cos(n\phi'/2), \quad (36)$$

where $r_{>}$ ($r_{<}$) is the larger (smaller) one of the two radial coordinates r and r' . One then gets an expression for the velocity potential in the form of Eq. (17), with $G(\vec{r}, \vec{r}')$ given by Eq. (36) and the $\vec{v}_0 \cdot (\vec{v}_0 \cdot \nabla) \vec{v}_0$ evaluated from Eqns. (34) and (35). Taking then the gradient, the correction to the velocity field is calculated. In our subsequent calculations, we introduce a radial cutoff, which we take to be $0.1a$, to exclude the small r region where[20] the zeroth order velocity has a weak square root singularity.

In principle, this procedure involves no advanced mathematical steps. However, one can readily see that it is very lengthy and intricate. Since the right side of Eq. (17) is cubic in \vec{v}_0 , the components of which are in the form of a series, and the Green function Eq. (36) involves an additional sum, the expression has the form of a quadruple sum, plus integrals over the angle ϕ' and the radial coordinate r' . This is done analytically: the angular integrals are performed first and lead to Kronecker deltas that reduce the number of sums. The radial integrals are done next and finally, the remaining (convergent) summations are evaluated. The resulting expression, however, is much too involved to be written here, and it would be truly very difficult even to keep track of all the terms without the help of a symbolic package (we have used Mathematica). The results can then be plotted and the plots are much more illuminating than the lengthy expressions.

One can however see from the basic structure of the equations that overall \vec{v}_1 is proportional to the basic velocity scale of the system, which is Ωa , times a factor of $\lambda = (\Omega a / v_s)^2$ where $v_s^2 = 1/(\kappa \rho_0)$. It is rather obvious also from the equations that \vec{v}_1

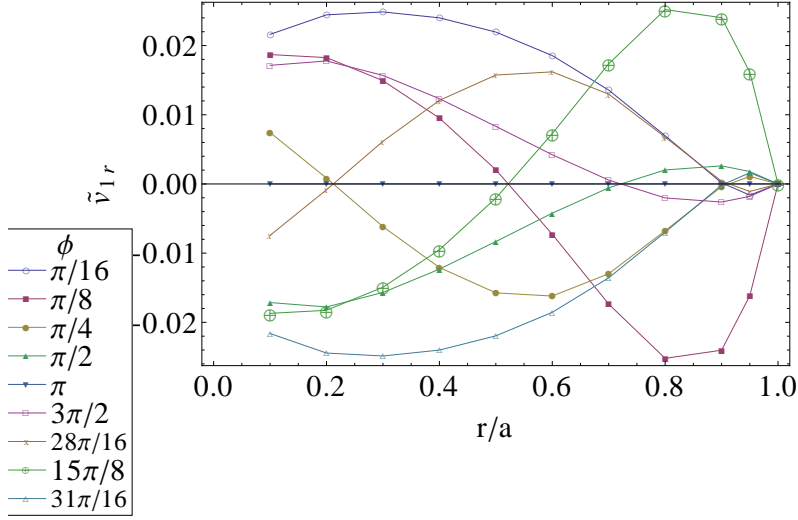


Figure 4. Plot of the radial component of the correction to the velocity field \vec{v}_1 for an obstructed cylinder. The dimensionless quantity shown is $\tilde{v}_{1r} \equiv v_{1r}/(\lambda v)$, plotted versus r/a at different angles ϕ .

has both radial and azimuthal components. Results for these components are shown in the next two figures. There, the dimensionless quantity plotted is a component of v_1 , divided by $\lambda\Omega a$. These are shown as functions of angle and dimensionless radial distance r/a .

In Figure 4 we present a plot of the radial component (v_{1r}) in the units described above, at several fixed values of the angle ϕ . One can see that the radial correction to the velocity field goes to zero at $r/a = 1$ satisfying the radial boundary condition discussed above. The magnitude of the correction to the radial velocity (v_{1r}) peaks at different values of r/a depending on how far one is from the line of obstruction along the azimuthal direction. At $\phi = \pi/8$, the peak in the magnitude of v_{1r} occurs closer to $r/a = 1$ than at $\phi = \pi/2$ where it occurs closer to the lower cut-off. At $\phi = \pi$, v_{1r} is identically zero owing to the symmetry of the problem over an angle of 2π . The corresponding azimuthal component ($v_{1\phi}$) is presented in Figure 5. The quantity $v_{1\phi}$ is now plotted in dimensionless units at several values of the dimensionless distance r/a . It can be seen that oscillations, in which one can discern traces corresponding to the $n = 3$ and $n = 5$ terms of the expression for $v_{0\phi}$ in Eq. (34), are present in the azimuthal correction to the velocity. This arises from the cubic (in v_0) nature of the perturbation. Again, the boundary conditions at $\phi = 0, 2\pi$ are satisfied with the velocity correction being zero at these values of ϕ .

Having calculated the correction to the velocity field due to finite compressibility, we can next study the correction to the density profile (ρ_1). This turns out to be computationally much simpler. Starting with Eq. (14), a line integral over $d\vec{r}$ enables us to calculate ρ_1 . Since the right side of Eq. (14) can be expressed as the gradient of a scalar quantity, doing an integral over \vec{r} ,

$$\int \nabla \rho_1 \cdot d\vec{r} = - \int \rho_0^2 \kappa (\vec{v}_0 \cdot \nabla) \vec{v}_0 \cdot d\vec{r} \quad (37)$$

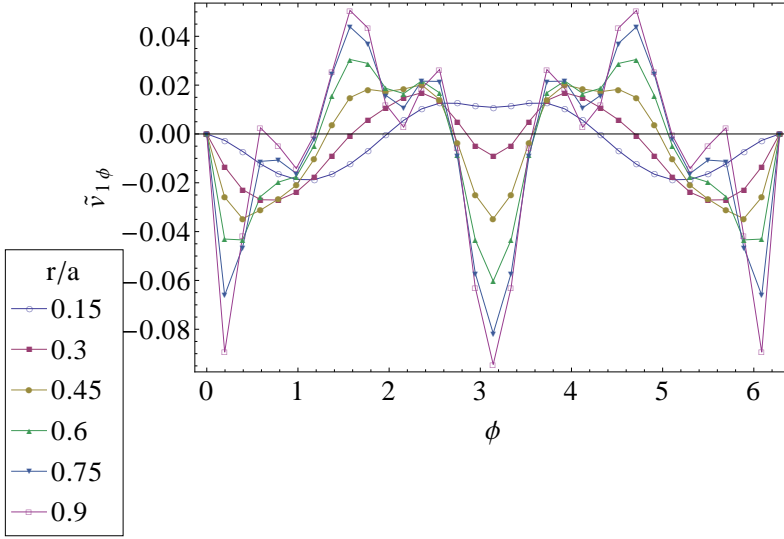


Figure 5. Plot of the azimuthal component of the correction to the velocity field \tilde{v}_1 . The dimensionless quantity shown is $\tilde{v}_{1\phi} \equiv v_{1\phi}/(\lambda v)$, plotted versus ϕ at different values of r/a .

enables us to calculate ρ_1 independent of the path chosen within the obstructed cylinder. Using this property of $\nabla\rho_1$, we calculate $\rho_1(r, \phi)$ from a line integral over two different paths and confirm that our result is indeed path independent. We determine the arbitrary constant associated with the integration by enforcing the condition that the total integral of ρ_1 over the relevant region be zero i.e. $\int \rho_1 r dr d\phi = 0$. This condition makes sense physically since the constraint imposed by the container implies that the total mass change due to the compressibility correction must be zero. This gives us the full function $\rho_1(r, \phi)$. Because of the nonlinearities in v_0 present in the equations, the results, although formally analytic in terms of convergent double series, are again quite intricate and will not be written down explicitly here. Instead, as before, results are plotted in the next two figures. The quantity plotted is the dimensionless $(\rho_1/(\rho_0\lambda))$ and we plot it at different values of ϕ in Figure 6. One can see that that radial dependence of the density correction is more prominent closer to the line of obstruction within the cylinder, which makes sense physically. Also, it is positive or close to zero near the outer boundary, and negative at smaller values of r/a . This seems to be a direct consequence of the fact that the higher the velocity of fluid flow, the lower is the condensate density [38]. Physically, the compressibility correction depletes the density at smaller values of r/a and, conversely, increases it at large values. Similarly, the azimuthal dependence of $\rho_1(r, \phi)$, is plotted at different values of r/a in Figure 7. The angular dependence of these results reflects again the nature of the perturbation.

We proceed now to analyze the order of magnitude of these corrections in typical cold atomic systems. For this problem (as opposed to the gaussian profile situation) the values of the dimensionless quantities plotted do not exceed unity, so that the corrections are now smaller and the perturbation theory is valid for larger values of λ . Our results show that compressibility corrections for fixed Ω are smaller for more confined geometries. In this case, it is best to phrase the issue in terms of the validity of

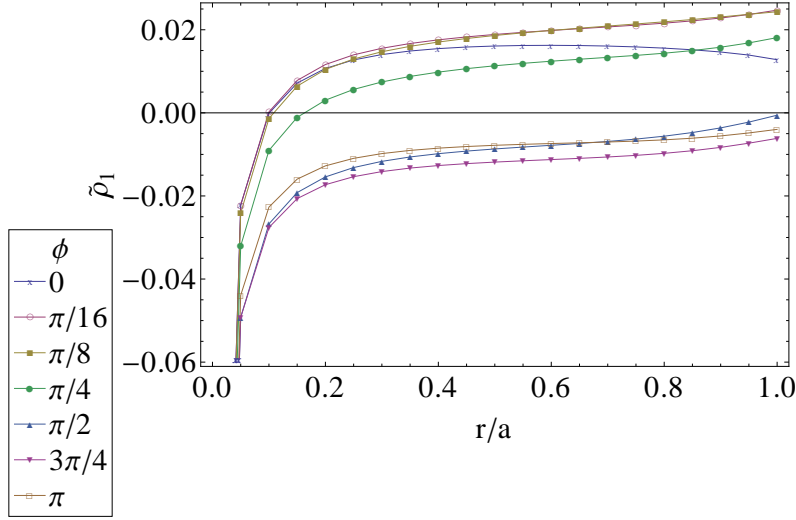


Figure 6. Plot of the radial dependence of the dimensionless correction to the density - $\tilde{\rho}_1 \equiv \rho_1/(\lambda\rho_0)$ - due to finite compressibility at different values of ϕ .

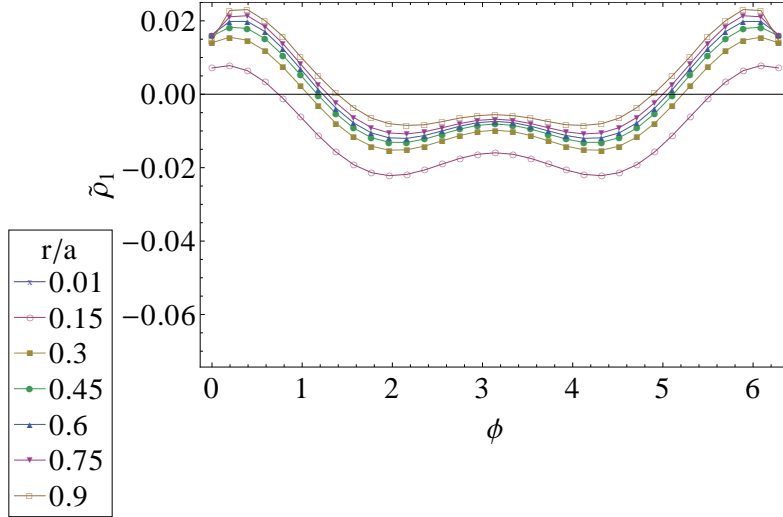


Figure 7. Plot of the azimuthal dependence of the dimensionless correction to the density - $\tilde{\rho}_1 = \rho_1/(\lambda\rho_0)$ - due to finite compressibility at different values of r/a .

the theory (or the need for it) in the upper part of the relevant range of Ω . This range of Ω values is limited by the requirement that the circulation created by the zeroth order velocity does not exceed a flux quantum. The velocities involved are roughly[20] of order $10^{-1}\Omega a$. Demanding then that this speed, times a , be of order of one flux quantum and using the order of magnitude values discussed previously, we find that the corresponding λ for cold atomic systems may reach values up to 10^{-2} . Thus, we find that for these systems finite compressibility corrections are not always negligible but on the other hand they are, at least for samples that are not too small, amenable

to our perturbation approach. For superfluid helium we find, as expected, that λ is much smaller and the incompressible limit calculations are perfectly adequate.

4. Conclusions

In this paper, we have studied, by means of an analytic method, the hydrodynamics of compressible superfluids in confined geometries. We have shown that for practical cases of interest in cold atomic systems confined to complex geometries the corrections to the zero compressibility results are not negligible, but they can in many realistic cases be treated in a perturbative manner with the relevant dimensionless parameter being the square of the ratio of the typical speed to the sound speed (the Mach number). This method may be used in very general situations. We have illustrated the procedure by working out two examples. In the first, confining forces that need not be specified constrict the fluid to having a Gaussian density distribution at zeroth order. In the second, we have considered the case of a rotating obstructed cylinder filled with superfluid, with the density being uniform when the cylinder is at rest. The zeroth order (incompressible limit) solution to the problem is available[20] and the perturbative method is used to evaluate the corrections, again essentially in an analytic way. The general usefulness of the method is therefore illustrated by these examples. The general nature of the perturbative method applied to superfluids in confined geometries makes it useful for describing the results of relevant experiments on cold atomic systems, some of which have been mentioned in the Introduction. One of the main advantages of our procedure is that, since the resulting equations are linear, it is very amenable to analytic solution. We expect that this method will complement numerical calculations based on more microscopic descriptions such as the GP equation. Starting directly from the hydrodynamic equations is, in the appropriate limit, a good alternative to using the full GP equations, for situations where a hydrodynamic scale flow is imposed on the system.

5. Acknowledgment

This research was supported in part by IUSSTF grant 94-2010.

6. References

- [1] W. Ketterle, D.S. Durfee and D.M. Stamper-Kum, arXiv/cond-mat/9904034 (1999).
- [2] F. Dalfovo, S. Giorgini, L. P. Pitaevskii and S. Stringari, Rev. Mod. Phys. **71**, 463 (1999); S. Giorgini, L.P. Pitaevskii and S. Stringari, *ibid* **80**, 1215 (2008).
- [3] O. Morsch and M. Oberthaler, Rev. Mod. Phys. **78**, 180, (2006).
- [4] R. Onofrio, C. Raman, J.M. Vogels, J.R. Abo-Shaeer, A.P. Chikkatur and W. Ketterle, Phys. Rev. Lett. **85**, 2228 (2000).
- [5] O.M. Marago, S.A. Hopkins, J. Arlt, E. Hodby, G. Hechenblaikner, and C. J. Foot, Phys. Rev. Lett. **84**, 2056 (2000).
- [6] C. Ryu, M.F. Andersen, P. Clade, V. Natarajan, K. Helmerson and W.D. Phillips, Phys. Rev. Lett. **99**, 260401 (2007).
- [7] K. W. Madison, F. Chevy, W. Wohleben and J. Dalibard, Phys. Rev. Lett. **84**, 806 (2000).
- [8] B. Clancey, L. Luo and J.E. Thomas, Phys. Rev. Lett. **99**, 140401 (2007).
- [9] A. Ramanathan, K.C. Wright, S.R. Muniz, M. Zelan, W.T. Hill III, C.J. Lobb, K. Helmerson, W.D. Phillips and G. K. Campbell, Phys. Rev. Lett. **106**, 130401 (2011).
- [10] R.B. Blakestad, C. J. Lobb, W. D. Phillips, and G. K. Campbell, Phys. Rev. Lett. **110**, 025302 (2013).
- [11] E. Kim and M.W.H. Chan, Science **305**, 1941 (2004).

- [12] For a review, see S. Balibar and F. Caupin, J. Phys. Condens. Matter **20**, 17320 (2008).
- [13] D. Kim and M. Chan, Phys. Rev. Lett. **109**, 155301 (2012).
- [14] L. Pollet, M. Boninsegni, A.B. Kuklov, N.V. Prokof'ev, B.V. Svistunov and M. Troyer, Phys. Rev. Lett. **98**, 135301 (2007).
- [15] M. Boninsegni, A.B. Kuklov, L. Pollet, N.V. Prokof'ev, B.V. Svistunov and M. Troyer, Phys. Rev. Lett. **99**, 034301 (2007).
- [16] A.T. Dorsey, P. M. Goldbart, and J. Toner, Phys. Rev. Lett. **96**, 055301 (2006).
- [17] C. Dasgupta and O.T. Valls, Phys. Rev. B **82**, 024523 (2010).
- [18] A. L. Fetter, J. Low Temp. Phys. **16**, 533 (1974).
- [19] A.L. Fetter, Phys. Rev. **152**, 183 (1966).
- [20] C. Dasgupta and O.T. Valls, Phys. Rev. E **79**, 016303 (2009).
- [21] D. E. Sheehy and L. Radzihovsky, Phys. Rev. A **70**, 063620 (2004).
- [22] A. L. Fetter, Rev. Mod. Phys. **81**, 647 (2009).
- [23] C.J. Pethick and H. Smith, *Bose-Einstein Condensation in Dilute Gases*, Cambridge University Press, Cambridge, England (2002).
- [24] See, for example, footnote [15] in S. Stringari, Phys. Rev. Lett. **77**, 2360 (1996).
- [25] Chi-Tuong Pham, Caroline Nore, M.-É. Brachet, Physica D: Nonlinear Phenomena, **210**, 203 (2005).
- [26] Sergio Rica, Physica D: Nonlinear Phenomena, **148**, 221 (2001).
- [27] V. Bretin, S. Stock, Y. Seurin, and J. Dalibard, Phys. Rev. Lett. **92**, 050403 (2004).
- [28] A. Aftalion and P. Mason, Phys. Rev. A **81**, 023607 (2010).
- [29] L. Rayleigh, *The Theory of Sound*, Macmillan and Co, London (1877).
- [30] C. Eckart, Phys. Rev. **73**, 68-76 (1948).
- [31] S. Inouye, S. Gupta, T. Roseband, A.P. Chikkatur, A. Gorlitz, T.L. Gustavson, A.E. Leanhardt, D.E. Pritchard and W. Ketterle, Phys. Rev. Lett. **87**, 080402 (2001).
- [32] R. Desbuquois, L. Chomaz, T. Yefsah, J. Leonard, J. Beugnon, C. Weitenberg and J. Dalibard, Nature Physics **8**, 645-648 (2012).
- [33] A.L. Fetter, C.J. Foot, [arXiv:1203.3183\[cond-mat.quant-gas\]](#) (2012).
- [34] See Page 89 in M. Ueda, *Fundamentals and New Frontiers of Bose-Einstein Condensation*, World Scientific Publishing Co., Singapore (2010).
- [35] James A. Joseph, PhD Thesis, Duke University, (2010).
- [36] J.C. Findlay, A. Pitt, H.G. Smith, J.O. Wilhelm, Phys. Review, **54**, 7 (1938).
- [37] See page 142 in J. D. Jackson, *Classical Electrodynamics*, 3rd Edition, Wiley, New York (1999).
- [38] C. Raman, M. Kohl, R. Onofrio, D.S. Durfee, C.E. Kuklewicz, Z. Hadzibabic and W. Ketterle, Phys. Rev. Lett. **83**, 2502-2505 (1999).